Clim. Past Discuss., 8, 1485–1522, 2012
www.clim-past-discuss.net/8/1485/2012/
doi:10.5194/cpd-8-1485-2012

Climate of the Past Discussions

Synoptic climatology and recent climate trends at Lake El'gygytgyn

M. Nolan[1], **E. Cassano**[2], **and J. Cassano**[2]

[1]University of Alaska Fairbanks Institute of Northern Engineering Fairbanks, AK 99775, USA
[2]University of Colorado at Boulder Cooperative Institute for Research in Environmental Sciences, 216 UCB Boulder, CO 80309, USA

Received: 2 March 2012 – Accepted: 16 March 2012 – Published: 23 April 2012

Correspondence to: M. Nolan (matt@drmattnolan.org)

Published by Copernicus Publications on behalf of the European Geosciences Union.

Abstract

We developed a synoptic climatology for Lake El'gygytgyn, Chukotka Russia, and explored modern climate trends affecting air temperatures there to aid in paleoclimate reconstructions of a 3.6 million year old sediment core taken from the lake. Our self-organized mapping (SOM) approach identified 35 synoptic weather patterns, based on sea level pressure, that span the range of synoptic patterns that influence the study domain over the 1961–2009 NCEP/NCAR reanalysis period. We found strong seasonality in modern weather patterns, with summer weather primarily characterized by weak low pressure systems over the Arctic Ocean or Siberia and winter weather primarily characterized by strong high pressures over the Arctic Ocean with strong low pressures in the Pacific Ocean. In general the primary source of variation in air temperatures came from the dominant patterns in each season, which we identify in the text, and nearly all of the dominant weather patterns here have shown increasing temperatures. We found that nearly all of the warming in mean annual temperature over the past 50 years (about 3 °C) occurred during sub-freezing conditions on either side of summer (that is, spring and fall). Here we found that the most summer-like weather patterns (low pressures to the North) in the shoulder seasons were responsible for much of the change. Finally we compared the warmest 15 years of the record (1995–2009) to the coolest (1961–1975) and found that changes in thermodynamics of weather were about 3 to 300 times more important than changes in frequency of weather patterns in controlling temperature variations during spring and fall, respectively. That is, in the modern record, general warming (local or imported) is more important by orders of magnitude than changes in storm tracks in controlling air temperature at Lake El'gygtgyn, and we conclude with a discussion of how these results may be relevant to the paleoclimate reconstruction efforts.

1 Introduction

Our goal in this work is to relate local weather to modern climate at Lake El'gygytgyn, Chukotka, Russia, to facilitate paleoclimate reconstructions of a 3.6 million year long core extracted there in 2009. We used the self-organized mapping (SOM) technique applied to the National Center for Environmental Prediction/National Center for Atmospheric Research (NCEP/NCAR) reanalysis data (Kalnay et al., 1996) from 1961–2009 to understand the modern synoptic climatology and its recent trends here. The physical characteristics of the lake, lake ice dynamics, core extraction, and interpretations of prior cores are all well described in a series of papers (Layer, 2000; Nolan et al., 2003; Brigham-Grette et al., 2007; Cherapanova et al., 2007; Glushkova and Smirnov, 2007; Melles et al., 2007; Minyuk et al., 2007; Nolan and Brigham-Grette, 2007; Juschus et al., 2011). The SOM technique (Kohonen, 2001) applied to synoptic climatology and reanalysis data is also well described (Kohonen, 2001; Reusch et al., 2005; Cassano et al., 2006; Schuenemann and Cassano, 2010) and our work here closely follows our use of SOMs in prior work (Cassano et al., 2011). This paper also draws heavily from a companion paper in this special issue (Nolan, 2012) which compares measurements from a local automated weather station (AWS) that we had running from 2002–2008 to the NCEP/NCAR reanalysis (also referred to herein as "NNR" or just "reanalysis") fields of air temperature, precipitation, and barometric pressure, and this information will not be duplicated here. Based on our prior comparisons of NNR air temperature with National Weather Service (NWS) stations throughout Alaska (Cassano et al., 2011) and with our local AWS at Lake El'gygytgyn (Nolan, 2012), we believe that NNR air temperature represents reality well at Lake El'gygtgyn and we have therefore used these data to analyze daily weather here without further reservation. Our goals in this paper are to understand the modern synoptic climate (1961–2009), determine which weather patterns bring warmer/colder air, help explain the large rise in mean annual air temperature seen within the NNR record here over the past 20 years (Nolan, 2012), and relate these results to paleoclimate.

CPD
8, 1485–1522, 2012

The SOM and daily lookup table we used here is exactly the same as we used in (Cassano et al., 2011), and the reader is referred there for details on our methods and parameter choices. The SOM technique is fully described in Kohonen (2001) and an overview of its applications to synoptic climatology is given in Hewiston and Crane (2002) and Cassano et al. (2007) but a short description is given here. The SOM technique employs a neural network algorithm that uses unsupervised learning to determine generalized patterns in data. For the work presented in this paper, daily sea level pressure (SLP) anomaly data are used to train the SOM to find the archetypical patterns that represent the weather patterns that influence the area of study. In the current work, a SOM with 35 patterns (7 columns by 5 rows) was used for analysis. SOMs of this size have been found suitable for synoptic climatology studies since this size SOM compactly displays the major circulation patterns and storm tracks (Hewiston and Crane, 2002; Cassano et al., 2007). Once the patterns have been identified, each day of data is compared with each pattern and it is associated with the pattern to which it is most closely matched. Numerous papers have shown the SOM technique to robustly identify the synoptic weather patterns that affect a given area (Reusch et al., 2005; Cassano et al., 2006; Lynch et al., 2006; Finnis et al., 2009; Schuenemann and Cassano, 2010). This list of dates associated with each pattern (the daily lookup table) can then be used in a variety of statistical ways. For example, annual or seasonal frequencies of each of the 35 patterns can be tracked with time, or another daily lookup table of air temperature anomalies can be compared to it to determine which patterns tend to bring the warmest or coldest weather. Figure 1 presents the master SOM from our prior work, reproduced here for convenience, which contains the 35 SLP patterns that we found characterize the domain, along with labels 1–35 corresponding to their identification in the text.

CPD
8, 1485–1522, 2012

2 SOM analysis of modern air temperature anomalies

We calculated mean air temperature anomalies for each SOM node to determine which patterns are responsible for bringing the warmest and coldest variations in local weather and then assessed whether these results matched our intuition about the dynamics responsible for those anomalies. To do this, we first calculated mean air temperature anomalies for each SOM node by reducing daily temperatures (Fig. 2a) to have zero-means by subtracting the mean temperature on, for example, 1 January from each of the 48 January 1sts in the period (Fig. 2a, first column) to arrive at a daily temperature anomaly on that day (Fig. 2b). Using the daily SOM lookup table we then took the mean of the daily temperature anomalies from 1961–2009 for all of the days represented by each pattern to arrive at a pattern-averaged temperature anomaly. Figure 3a shows an example of this for the NNR grid point closest to Lake El'gygytgyn. We did this for each grid point in the domain, allowing us to create spatial maps for each SOM pattern (Fig. 3b), which clearly illustrates the close relationship between circulation and temperatures in addition to how a particular weather pattern will affect each area of the domain. These anomaly maps largely eliminate seasonal trends (e.g., winter is colder than summer), though these trends are discussed in the next section.

As with all SOM analyses, conclusions made from an analysis product such as Fig. 3 is done by comparison with the SOM master plot in Fig. 1. For example, the warmest anomaly found in Fig. 3a, 4.9 °C, occurs at Pattern 26 (row 1, column 6). According to Fig. 1, Pattern 26 is characterized by a strong low pressure in the Bering Sea, south of Lake El'gygytgyn, and a strong high pressure in the Beaufort Sea to the north and east of the lake. In this situation, warm air from the south and east is funneled to the northwest between these two system. According to Fig. 3b, this pattern tends also to warm western Alaska with the same air, but cools western Canada by bringing cold Arctic Ocean air downwards on the eastern-side of the high pressure system.

The patterns that bring the warmest temperature anomalies to Lake El'gygytgyn also affect large regions of eastern Siberia and western Alaska. In general these are

CPD
8, 1485–1522, 2012

westward and northwestward shifted Aleutian Lows (Patterns 16, 21, 26, and 31) bringing air from the south and east. Other patterns that bring weaker warm temperature anomalies are those with weaker pressure systems in similar locations, bringing air from the south and east towards the northwest (Patterns 10, 15, and 20). Though the flows into the Lake are similar with these two clusters of patterns, the impact on Alaska is different as the latter tend to also bring cold air from the north and east to Alaska since for these patterns the high pressure in the Arctic Ocean is located further west putting Alaska in the northerly flow ahead of the system.

The coldest temperature anomalies for the Lake El'gygytgyn region are associated with moderate low pressure systems centered in the Gulf of Alaska with broad high pressure over eastern Siberia and the Beaufort/Chukchi Seas (Patterns 24–25 and 29–30). These patterns tend to bring air to the Lake from the east-northeast over the Arctic Ocean. When these patterns occur during the winter, the air advected into eastern Siberia likely passes over sea ice rather than open water and thus stays cold. When there is open water present, this may warm the air somewhat before reaching the Lake El'gygytgyn area. These patterns tend to cool all of Beringia, while warming Canada.

Analysis of Fig. 3b demonstrates the close linkages between 2 m air temperature anomalies and circulation patterns within the domain, which we believe strengthens all of the conclusions of this paper. For example, in Pattern 31 (row1, column 7), there is an Aleutian Low centered near the tip of the island chain with high pressure located in the Beaufort Sea. The distribution of temperature anomalies for this pattern show warm temperature anomalies over much of Siberia and Alaska in the southerly flow ahead of the low, and cold temperature anomalies in northwestern Canada in the northerly flow ahead of the high pressure system. In almost all cases, as expected, southerly flow ahead of low pressure systems moving west-to-east brings warm weather ahead of their approach and the converse, northerly flow ahead of a high pressure system, brings cold temperature anomalies to that area. Given that our local AWS data closely tracks the NCEP 2 m air temperatures (Nolan, 2012), and that

CPD
8, 1485–1522, 2012

the model's air temperatures and sea level pressure patterns closely track as we have just described, we believe the air temperature analyses we perform through this paper are accurate and appropriate for allowing a better understanding of modern local climate and its trends, and hope that this will be of use to the paleoclimate reconstruction effort. Our methods will hopefully make clear what teleconnections exist between Lake El'gygytgyn and the surrounding domain and how to exploit them, such as through comparisons with other paleoclimate sites within the domain.

3 Seasonal air temperature trends in SOM patterns

To expand upon our prior work which used calendar months to define seasons, here we explored the use of positive and negative degree days (PDD and NDD) to define seasons and trends. Degree days are defined by simply summing daily average air temperatures in °C. The motivation for using DD to define the freezing and thawing seasons is that nearly all biological and physical processes of interest to our core interpretations are strongly controlled by the liquid/solid transition of water, whether that be lake ice dynamics, soil erosion, vegetation growth, or aquatic biologic productivity. Further, DD themselves are especially useful metrics for determining lake ice thickness and timing of melt, and by tracking the transitions from freezing to thawing conditions by where the air temperature crosses the 0 °C threshold (which also separates PDD from NDD) we can also track changes in seasonal lengths, something not possible with calendar definitions of seasons. To begin, we start with only two seasons, a freezing and thawing season, and then later expand this to consider spring and fall dynamics.

We found strong seasonal trends in synoptic weather patterns, in terms of DD and wind direction, which may be of relevance to core proxies. Figure 4a and b plots the frequency of each weather pattern, in average number of days per year over 1961–2009, for the long-term freeze and thaw seasons defined above simply by air temperature. These figures show that freeze season is long and the thaw season is short, and that patterns with strong low-pressure centers over the Aleutians (right side of Fig. 1) dominate almost half the year on average. These systems both tend to bring cold air from the east and north to the Lake from areas dominated by snow-covered land or ice-covered ocean but rarely open ocean. However, these Aleutian Lows occur primarily in winter. The seasonal differences are strong, as almost any weather pattern can be expected for a few days in winter, but in summer the observed patterns are largely those lacking a strong low pressure in the Pacific. The patterns that do occur in the summer are characterized by low pressure systems much weaker than in winter and broad high pressures systems, which usually tend to bring warm air from ice-free areas of the Pacific from the south and west. What is not clear from Fig. 4 is the DD magnitude of these events. That is, one cannot make the claim that because a pattern is more frequent that it is more important to accumulating DD or to trends in PDD or NDD. For example, a pattern that occurs frequently but has a daily average DD near zero would contribute little to the annual total of DD, while a less frequent pattern with a large positive or negative DD, but that occurs less frequently, would contribute more to the annual total of DD.

While in general the bulk of the DD come from the most frequent patterns, some patterns stand out in magnitude and variation and have greater influence on lake weather. Figure 5a and b reveals which SOM patterns are most responsible for NDD and PDD. Here we find that NDD (4802 DD) is about 7 times higher than PDD (675 DD), meaning that summers are cool but winters are cold, and thus that winter (and winter weather patterns) dominate the annual DD signal (see Nolan, 2012 for more detail on this). Comparison of Figs. 4 and 5 reveals a major benefit of characterizing weather patterns by degree days, in that DD are the product of frequency and temperature, giving a sense of the actual magnitude of impact of a given pattern on seasonal temperature trends. In summer we find that frequencies and DD paint essentially the same picture, though minor differences are evident on the scale of several degree-days. The most important weather pattern in summer is represented by Pattern 1, characterized by low pressure centers north of the lake, with a mean PDD contribution of 66 and a standard deviation of about 40 DD. This variation is not large in an absolute sense, but

CPD
8, 1485–1522, 2012

it is larger than the standard deviation of annual PDD over the entire record (Nolan, 2012), indicating that this pattern alone could account for any inter-annual variations in summer PDD. In winter, however, the differences between frequency and magnitude are even larger. For example, Patterns 21 and 32 both have the same average frequency (Fig. 4), but differ by 107 DD (which is 15 % of the total PDD) in Fig. 5. Large discrepancies can be seen for several other patterns. Color in Fig. 5 represents the standard deviation of DD for each pattern and we can see that some patterns have a much higher variability than others. These weather patterns tend also to have the highest means and thus exert the strongest controls on their respective seasons as well as the strongest inter-annual variability. That is, inter-annual consistency drives seasonal processes, but inter-annual inconsistency drives variations and trends, and some patterns seem responsible for both. For example, we can see in winter that Patterns 5 and 30 occur with about the same frequency and magnitude, but that Pattern 5 has 50 % higher variation and thus more influence on whether a particular winter is warmer or colder. In this case, these two patterns alone account for about 10 % (542 DD) of the mean annual NDD, with a combined 2-sigma variation of about ±500 DD. Pattern 34 alone can vary from +45 to −547 DD (mean ± 2-sigma). Patterns 32, 33, and 35 also show high magnitudes coupled with high variability. These patterns are the real weather makers at Lake El'gygytgyn, at least in the modern environment.

4 Interannual air temperature trends in SOM patterns

The largest trend in air temperature over the modern record is the large increase in mean annual temperature (MAAT) begin in the late-1980s, from a 1961–1994 mean of −12.8 °C to a 1995–2009 mean of −9.1 °C (see Fig. 5 in Nolan, 2012), which we explained as being due to winter warming, with mean annual NDD rising from −5043 to −4340 DD over that same time. In this section we explore the changes in weather patterns that accompanied this change in MAAT using further DD analysis combined with SOM techniques.

Figure 2a–b shows daily NCEP air temperature and air temperature anomaly for the entire record (1961–2009), giving us a visual impression of those trends, especially in terms of defining spring and fall transitional seasons. In Fig. 2a, we can see beginning in the late-1980s that daily spring temperatures rose considerably, beginning in March (i.e., ~Days 60 to 90), and also that peak winter temperatures were warmer as well; the period 1995–2001 was especially notable for this. Fall also became warmer at this time, extending through 2009. Early summer, about Day 150, seems to have gotten a bit cooler about this same time, with late summers getting warmer. During this time, there was little trend in PDD, with means changing from +666 to +700, indicating that the changes largely balance out in terms of PDD. Given this visual inspection, it seems that the calendar month definition of spring and fall (MAM and SON) are reasonable fits for exploring frequency and magnitude changes at the lake, but obviously cannot help us with changes in season lengths. For example, in Fig. 8b of Nolan (2012), we showed that the length of thaw season increased by over 3 weeks between 1961–2009, largely due to delayed fall. These changes in air temperature are perhaps shown more clearly in Fig. 2b which plots air temperature anomalies (defined previously); daily air temperature anomalies are equivalent to degree day anomalies. By mapping these DD anomalies to the SOM weather pattern corresponding to that day, we can begin to look at these temperature trends as attributable to their synoptic-scale drivers.

By plotting DD for each SOM pattern for each year, we can explore the causes of warm and cold years. Figure 6a and b do this for PDD and NDD respectively. These plots also give a graphic representation of which patterns dominate which season; for example, Patterns 20–35 clearly contribute little to summer heating, but dominate winter cooling. In Fig. 6a, we see that Pattern 1, 3, and 8 largely explain the highest PDDs on record in 1991. Similarly, an unusually high PDD in Pattern 1 in 2002 and 2003 largely balance cooling seen in some of the others, and in 2004 a record high Pattern 2 dominated moderate warming of other cells to create the record high annual PDD. In the freezing seasons (essentially fall, winter, and spring), Patterns 5 and 30–35 show the high inter-annual variability, as also seen in Fig. 5, with most patterns showing

CPD
8, 1485–1522, 2012

some warming over time. Note again that the magnitude of variation is much higher in the freeze season than in the thaw season, indicating that below-freezing weather has the most potential for changing annual means at Lake El'gygytgyn.

We analyzed trends in DD for each of the 35 patterns by fitting linear trend lines through their annual DD from 1961–2009. An example of this analysis is presented in Fig. 7a for Pattern 6. Here we see a strong rise in DD over time, seemingly characteristic difference between the first and last 15 years of the record, and a general switch from being a contributor to NDD to PDD. In Fig. 7b the magnitude of change over the analysis period (that is, the difference in trend line endpoints such as in Fig. 7a) is shown as text, with those patterns changing from negative to positive DD (like in Fig. 7a) in thick boxes, and the cell color representing positive and negative DD for 2009 for reference. We find that nearly all patterns have shown warming over this time, some patterns have changed from contributing to PDD from NDD, and some patterns emerge as driving overall change. The general picture that emerges here is that the patterns that are showing the most warming are not those characteristic of the freezing season (right side in Fig. 1), but those characteristic of thawing season (upper left in Fig. 1) that occur during the freezing season. However, the thaw season is not getting warmer, but rather the *freezing-season occurrence* of typical thaw-season patterns are getting warmer and, perhaps more importantly, these patterns are often crossing or approaching the transition from being net NDD-contributors to net PDD-contributors. Winter-only patterns, such as the Aleutian Lows, are also getting warmer, but with a few exceptions lower in magnitude and lower in percentage change in DD than the summer-like patterns. Perhaps more importantly for our paleoclimate purposes, none of these freezing-season patterns is close to crossing the 0 DD threshold. Thus it seems that the warmest of the winter patterns are experiencing the most change, and these are of course found at the transitions between winter and summer; that is, fall and spring, as we saw in Fig. 2.

Analysis of annual trends in seasonal DD further confirms that much of the recent warming can be explained by changes in spring and fall. Here we defined winter,

CPD
8, 1485–1522, 2012

spring, summer, and fall by the standard 3 month intervals of DJF, MAM, JJA, and SON, respectively (where the letters are the initial of each month); note also that for convenience DJF values were all calculated from the same calendar year, rather than December of the prior year, largely for numerical convenience and spot checks confirmed this made no difference to our conclusions. Figure 8 shows that most of the change in fall and spring appears to have occurred starting about 1995, when mean negative DD appear to have to increased by 286 DD and 339 DD, respectively, more than 2 standard deviations above their prior means. The remaining NDD from the winter season (DJF) shows essentially no jump or trend indicating that nearly all MAAT increase is being driven by warming springs and falls. Further, nearly all of the trend in mean-annual PDD (+34 DD) after 1994 can be explained by warming falls, which increased in means by +31 DD after 1994.

5 Interdecadal air temperature trends in SOM patterns

Given that weather here seems to have changed around 1995, and that we have 15 years of such data (1995–2009) following this that approach "climate" time-scales, we chose to compare this period to the first 15 years (1961–1975) of the record. The DD trend *during* both of these periods is near zero, suggesting that these are periods of relatively stable, but different, climate. Some of the intervening years show signs of being intermediate between the two states, further influencing our choice of comparison periods. We calculated degree days for each period, pattern, and season by taking the mean of the 15 seasonal values calculated by summing daily values within that season for each year. Then we differenced the values between periods for each season, plotting the results in Fig. 9 with numbers indicating the change in DD with numbers and representing the magnitude of DD in the first period with colors to visualize the seasonal importance of each pattern. The total annual change was +886 DD and per season was +31, +338, +318, and +199 DD for the JJA, MAM, SON, and DDJ periods respectively, further indicating spring and fall (MAM and SON) as the primary

CPD
8, 1485–1522, 2012

drivers of annual change in the modern record. Note that the spring and fall periods are characterized by sub-freezing temperatures, so these total DD changes are over 95 % due to changes in NDD.

Interesting trends for individual weather patterns are also apparent within each season (Fig. 9). Most of the change in summer is coming from those patterns that are most frequent (as seen in Fig. 4), as we described previously, but several summer patterns actually show slight cooling. The largest changes in fall are from those patterns typical of summer (upper left corner in Fig. 9c), which are characterized by low pressure systems over the Arctic Ocean. In fall, these patterns still bring freezing air temperatures, but the air is warmer now than earlier in the record, suggesting that fall is becoming more like summer. Typical winter patterns that occur in fall (right side of Fig. 9d) characterized by strong Aleutian Low pressure centers also show warming in fall, as does Pattern 16 which has a strong low pressure center south of Chukotka. Thus in fall, patterns bringing winds from nearly every direction show warming, though the summer-like Pattern 1 shows the highest increase. In spring, the biggest changes are found in those patterns that are characteristic of spring (as denoted by color in Fig. 9b), which are intermediate between summer and winter patterns characterized by weak low pressure centers near the Aleutians and even weaker high pressure centers in the Arctic Ocean. Almost all patterns in spring show warming as well. In winter, the bulk of the change appears to be coming from patterns that do not typically dominate the winter climate. That is, other than Pattern 35 (a strong low pressure in the Gulf of Alaska and the strongest high pressure in the Arctic Ocean), the typical winter patterns show relatively little change. The biggest changes in winter are seen in patterns characterized by high pressures over Chukotka (e.g., Patterns 3–5, 10) and those with strong low pressures over or below Chukotka (e.g., Patterns 16, 17, 21). Overall, as the DD numbers show, all seasons show warming, and most patterns show warming with all of the largest magnitudes being positive.

CPD
8, 1485–1522, 2012

6 Attribution of air temperature trends in SOM patterns

What is the cause of the seasonal warming trends? We decided to use the SOM technique to investigate whether this climate shift was due to a change in frequency in weather patterns towards those that bring warm weather or whether some patterns are simply getting warmer without becoming more frequent, as we had done in prior work (Cassano et al., 2011). This SOM analysis is nearly identical to this prior work which explored a shift in climate from 1961–1975 to 1976–1990 that strongly affected air temperatures throughout much of Alaska, just relabeled here in terms of DD. This shift in 1976 does not appear as strongly at Lake El'gygytgyn, if at all, and here the period 1976–1993 shows signs of being a transition between the two periods we chose for our new study. We also extend our analyses here to understand the seasonal differences in this shift. For clarity, we summarize the basic mathematics here. We start by calculating a mean frequency (in days per year) and a mean temperature for each pattern for each time period (1961–1975 and 1995–2009), calling them F_{1i}, F_{2i}, T_{1i}, and T_{2i}, respectively, where the i represents each of the 35 weather patterns in the SOM. We can then calculate mean DD for each period for each pattern by

$$\mathrm{DD}_1 = \sum^{i=1:35} (F_{1i} * T_{1i}), \tag{1}$$

and

$$\mathrm{DD}_2 = \sum^{i=1:35} (F_{2i} * T_{2i}) \tag{2}$$

F_2 and T_2 can also be described as:

$$F_{2i} = F_{1i} + \Delta F_i, \text{ where } \Delta F_i = F_{2i} - F_{1i} \tag{3}$$

and

$$T_{2i} = T_{1i} + \Delta T_i, \text{ where } \Delta T_i = T_{2i} - T_{1i} \tag{4}$$

CPD
8, 1485–1522, 2012

Substituting Eqs. (3) and (4) into Eq. (2). Subtracting Eq. (2) from Eq. (1), and recombining terms yields

$$\mathrm{DD}_2 - \mathrm{DD}_1 = \Sigma(F_{1i} * \Delta T_i + T_{1i} * \Delta F_i + \Delta T_i * \Delta F_i) \quad (5)$$

Thus the total change in degree days can be split between the three terms at right. The first term (F_{1i} * ΔT_i) represents the component of DD change between periods that would have occurred if the frequency of the 35 weather patterns stayed constant in time. In this case, any non-zero change would have to come from an increase in air temperature associated with that pattern, such as a warming of the source area from which the winds advect air. The second term (T_{1i} * ΔF_i) represents the component of total change assuming that the mean temperature of each pattern stayed constant in time, and all non-zero change resulted from a change in frequency of a pattern. This would be the case if the thermodynamics of the patterns had not changed at all, but simply a shift in their relative frequencies. For example, if a pattern that typically brings warm air became more frequent at the expense of a pattern that bought cooler air (in the first period), total degree days would increase due to this term. The final term (ΔT_i* ΔF_i) describes the impact of both frequency and thermodynamics changes that occur together, and it is usually minor compared to the other terms (Cassano et al., 2011). The result of this analysis is shown in Table 1.

Changes in thermodynamics of patterns (887.2 DD) dominate the total change in degree days, as seen in Table 1, with most of that change occurring in spring and fall (341.8 and 324.3 DD, respectively). Here changes in thermodynamics range from 3 to 295 times the magnitude as changes in frequency, with the largest values in spring and fall. The clear picture that emerges from our research is that the warming observed in the NCEP/NCAR reanalysis mean annual air temperatures at Lake El'gygytgyn is caused by changes in thermodynamics of weather patterns, mostly in spring and fall, not from changes in their relative frequencies.

We plotted change in frequency between periods in Fig. 10 and confirm that these changes are relatively small. Here we plot the change in average number of days

CPD
8, 1485–1522, 2012

per period that each SOM pattern appears in the record. Most changes are 1 day or less between periods, with seasonal standard deviations (across all SOM Patterns) of 0.75, 0.72, 0.60, and 0.85 days for spring, summer, fall, and winter respectively (all are zero mean change because one pattern must be replaced by another). Some of the largest changes, 1.5 to 2 days, occur in winter, but as a percentage change these are some of the lowest. Percentage change can be estimated by comparing the colors in Fig. 10, which represent pattern frequency during the first period, to the numbers, which is the change between the two periods. For example, even though Pattern 35 changed by −1.9 days in winter (Fig. 10e), given that its older frequency was about 5.8 days per year, the percentage change is about −33 %. Similarly, Pattern 2 increased by 0.3 days in winter, but averaged only about 0.3 days in the first period, for a change of about 100 %. The largest frequency changes in summer occurred, for the most part, to those patterns that were already the most frequent. Fall showed the lowest standard deviations in magnitudes, but some of the highest percentage changes. In general, however, frequency changes were small between these time periods and further confirm our conclusions from Table 1 that changes in frequency between patterns are *not* responsible for the bulk of the warming we see in degree days during this time.

Where is this warmer air coming from? Our analysis does not distinguish between local warming and warming advected from elsewhere. In our prior work looking at climate changes in Alaska around 1976, because temperatures jumped 3–5 °C in a year within a longer-term cooling trend, it seemed reasonable to believe that the bulk of the warm air was coming from non-local sources. In that case, patterns dominating change had winds from the south, suggesting Pacific Ocean source. At Lake El'gygytgyn, the warming is more gradual, which may indicate that local warming is more important here than the 1976 shift in Alaska, a jump that was not observed at the lake. Based on Fig. 9 there is no clear picture of where any non-local warmer-air is sourced from, but generally it is mostly from the west, south, and east. In fall, the biggest increase is in Pattern 1, which has air largely coming from the west, over continental Russia,

CPD
8, 1485–1522, 2012

Title Page
Abstract | Introduction
Conclusions | References
Tables | Figures
◂◂ | ▸▸
◂ | ▸
Back | Close
Full Screen / Esc
Printer-friendly Version
Interactive Discussion

and the second biggest increase is Pattern 16 coming from the south, over the Bering Sea. In spring, the biggest increases comes from Patterns 28, 23, 19, and 20, which all tend to bring air from the east, over continental Alaska, or from the north over the Arctic Ocean. Given this, a warming Alaska or a decreasing trend in sea ice extent could have some influence on Siberia. In any case, the lake climate-trend story here seems more complicated than the 1976 story in Alaska, but the overall picture is similar in that the cause is a change in thermodynamics of patterns rather than an increase in frequency of patterns which typically bring warm air.

7 Relevance to paleoclimate

We believe that exploring trends in modern weather is important for paleoclimate studies because these trends give us our only direct evidence as to which patterns are most variable as well as the nature of this variability, with the implicit assumption being that the same may have been true in the past. At Lake El'gygytgyn, this assumption is more likely to be true over the most recent part of the sediment core record, as the influence of plate tectonics on climate begins playing a role in the older part. Similarly, the range of weather patterns we see today may not be the same as those during glacial times, when sea level was much lower and the ocean currents much different. So our results here are likely to better inform paleoconditions during *interglacials* of the past 1 M year, when circulation patterns were likely most similar to today. Unfortunately, given that much of the recent warming over the past 50 years was due in part to anthropogenic influences, we cannot be certain that the dynamics we observe now are representative of prior interglacial periods either. However, given the modern instrumental period of the 50–100 years is the only direct measure we have, we feel our analyses here are getting us pretty close to the best use of it possible for paleoclimate reconstructions, and we believe that this understanding of the modern environment and its trends should provide some calibration for the dynamics of modern proxies and thus hopefully improve the paleo-proxy development through comparison.

CPD
8, 1485–1522, 2012

Synoptic climatology and recent climate trends at Lake El'gygytgyn

M. Nolan et al.

In terms of core proxy interpretation, perhaps the most relevant finding (beyond the obvious that winters are long and cold) is that summer weather tends to come from the south and west and winter weather tends to come from the north and east, as this may relate to isotopic and other chemical indicators of provenance; that is, wind-blown or affected proxies indicating an origin in the south could perhaps also now be used as indicators of warmer weather. Given that winters dominate the mean annual air temperatures here, winters also have the largest potential for variation. We found very little change in summer temperatures over the past 50 years, but we did find an increase in winter's negative degree days by an amount *greater than the total mean summer positive degree days*. Thus, all else being equal, when interpreting proxy temperatures for mean annual temperatures, the freezing season, and in particular the shoulder seasons of spring and fall, should be considered as the most likely source of variation.

We also found that weather patterns here seem relatively stable with time, showing little change in frequency compared with changes in what those patterns bring with them. Given that some of the largest changes in global temperature in the past few thousand years have occurred during this 50-year interval, we have some confidence that the range of weather patterns that existed during this interglacial and many recent ones is captured by those of the past 50 years and that their frequency during interglacials was likely similar. Thus, when interpreting air temperatures changes here in prior interglacials, based on this analysis one should probably look to changes in thermodynamics first rather than a shift in frequency of storm tracks.

While nearly all of the change we found occurred during the freezing season, specifically these changes were found at the shoulder seasons to summer – spring and fall. We found little change in summer itself, in terms of DD or frequency. Fall weather patterns are getting warmer primarily through the variations of typical summer patterns that occur in fall. These patterns are not getting more frequent, but rather the source area for wind advection is getting warmer. In this case, the source area is largely from the southwest from continental Russia. However, nearly all patterns showed warming,

Discussion Paper | Discussion Paper | Discussion Paper | Discussion Paper |

CPD

8, 1485–1522, 2012

Synoptic climatology and recent climate trends at Lake El'gygytgyn

M. Nolan et al.

with wind therefore coming from every direction, and confusing things further is that our methods do not distinguish advected warming from local warming. So the picture of warming here is less clear than the warming that Alaska experienced after 1976, and therefore proxy interpretations will require some care when evaluating our work relative to source area effects of proxies.

The thaw season is important to nearly all physical and biological processes of interest at the lake, yet how summers change is largely unresolved by our work because we did not observe much change in the past 50 years. Our results do hint at a mechanism, however, that may help us understand how summers got cooler in the past to create multi-year ice covers (Nolan, 2012). We saw that fall is getting warmer because its summer-like patterns are bringing warmer air, and that this is having the effect of increasing thaw season length, so we know that these patterns are susceptible to significant changes. But since these summer-like patterns did not change much in *summer*, it may be that they have reached an upper limit of change (e.g., an equilibrium has been reached with the source region air), implying it is only possible for these patterns to get cooler at this point (e.g., by bringing less warm air in), at least within the summer season. In the shoulder seasons, having not reached this upper limit or equilibrium, they are showing the most change of any patterns. So it could be that some or much of the cooling we know occurred in paleo-summer PDD was caused by shortening of the summer-season length due to colder summer-like patterns in fall and spring, rather than simply a decrease in peak summer temperatures. That is, in the modern environment, if increases in positive DD are at least partly controlled by the length of summer, and length of summer is in turn dictated by the warmth of air advected by summer-like patterns in spring and fall, it therefore seems reasonable to us to believe the converse – that the decreases in positive DD could be caused by cooling of this source region not just in summer but in spring and fall as well, as least for the several patterns in common over these three seasons. Exploring this further will require larger model domains and likely some weather-scenario testing within a climate model, but in any case it seems a reasonable first assumption to consider that because summers are so short and cold

CPD
8, 1485–1522, 2012

and that they showed little change in the modern environment despite strong annual warming, that the dynamics of change in paleo-summers was likely similar to that of modern summers, with changes in thermodynamics of the shoulder seasons leading to the majority of variation.

How representative is weather at Lake El'gygytgyn to its surroundings? Do patterns that tend to bring anomalously warm/cold air to Lake El'gygytgyn also bring warm air to elsewhere in Siberia or to other paleoclimate coring sites? The general pattern within the domain is similar to that of Lake El'gygytgyn, that the largest temperature anomalies (both warm and cold) occur in winter, as seen on the lower row and right sides of Fig. 3b. Note that this is not to say that the Lake El'gygytgyn region is representative of weather in Alaska, only that winter shows substantially more variability than summer in both. Indeed, most strong negative temperature anomalies are associated with strong positive temperature anomalies elsewhere in the domain, and vice versa. While it is clear that there is substantial spatial variability in climate and its trends within this domain, the differences are not random and our analysis has shown a way to deconstruct it in a straightfoward and reliable way that matches our intuition about winds from the north being colder than winds from the south. Thus we believe that these tools can be used in future studies to relate the Lake El'gygygytgyn paleoclimate reconstruction with similar ones from different locations.

Acknowledgements. This work was supported by NSF Grant EAR-0602512; note that any opinions, findings, and conclusions or recommendations expressed in this paper are those of the authors and do not necessarily reflect the views of the National Science Foundation, other funding sources, or any of the other team members. We would also wish to the thank the Lake E'gygytgyn science team for their support and numerous discussions about this project.

References

Brigham-Grette, J., Melles, M., Minyuk, P., and Party, S.: Overview and significance of a 250 ka paleoclimate record from El'gygytgyn Crater Lake, NE Russia, J. Paleolimnol., 37, 1–16,

2007.
Cassano, E. N., Cassano, J. J., and Nolan, M.: Synoptic weather pattern controls on temperature in Alaska, J. Geophys. Res., 116, D11108, doi:10.1029/2010JD015341, 2011.
Cassano, E. N., Lynch, A. H., Cassano, J. J., and Koslow, M. R.: Classification of synoptic patterns in the western Arctic associated with extreme events at Barrow, Alaska, USA, Clim. Res., 30, 83–97, 2006.
Cassano, J. J., Uotila, P., and Lynch, A. H.: Changes in synoptic weather patterns in the polar regions in the twentieth and twenty-first centuries, Part 1: Arctic, Int. J. Climatol., 26, 1027–1049, 2006.
Cassano, J. J., Uotila, P., Lynch, A. H., and Cassano, E. N.: Predicted changes in synoptic forcing of net precipitation in large Arctic river basins during the 21st century, J. Geophys. Res., 112, G04S49, doi:10.1029/2006JG000332, 2007.
Cherapanova, M. V., Snyder, J. A., and Brigham-Grette, J.: Diatom stratigraphy of the last 250 ka at Lake El'gygytgyn, northeast Siberia, J. Paleolimnol., 37, 155–162, 2007.
Finnis, J., Cassano, J. J., Holland, M. M., and Serreze, M. C.: Synoptically forced hydroclimatology of major Arctic watersheds in general circulation models, Part 1: the Mackenzie River basin, Int. J. Climatol., 29, 1226–1243, 2009.
Glushkova, O. Y. and Smirnov, V. N.: Pliocene to Holocene geomorphic evolution and paleogeography of the El'gygytgyn Lake region, NE Russia, J. Paleolimnol., 37, 37–47, 2007.
Hewiston, B. C. and Crane, R. G.: Self-organizing maps: applications to synoptic climatology, Clim. Res., 22, 13–26, 2002.
Juschus, O., Pavlov, M., Schwamborn, G., Federov, G., and Melles, M.: Lake Quarternary lake-level changes of Lake El'gygytgyn, NE Siberia, Quarternary Res., 76, 441–451, 2011.
Kalnay, E., Kanamitsu, M., Kistler, R., Collins, W., Deaven, D., Gandin, L., Iredell, M., Saha, S., White, G., Woollen, J., Zhu, Y., Leetmaa, A., Reynolds, B., Chelliah, M., Ebisuzaki, W., Higgins, W., Janowiak, J., Mo, K. C., Ropelewski, C., Wang, J., Jenne, Roy, and Joseph, Dennis: The NCEP/NCAR 40 year reanalysis project, B. Am. Meteorol. Soc., 77, 437–471, 1996.
Kohonen, T.: Self-organizing maps, New York, Springer, 2001.
Layer, P.: Argon-40/Argon-39 age of the El'gygytgyn impact event, Chukotka, Russia, Meteorit. Planet. Sci., 35, 591–599, 2000.
Lynch, A. H., Uotila, P., and Cassano, J. J.: Changes in synoptic weather patterns in the polar regions in the twentieth and twenty-first centuries, Part 2: Antarctic, Int. J. Climatol., 26,

1181–1199, 2006.
Melles, M., Brigham-Grette,J., Glushkova, O. Y., Minyuk, P. S., Nowaczyk, N. R., and Hubberten, H. W.: Sedimentary geochemistry of core PG1351 from Lake El'gygytgyn – a sensitive record of climate variability in the East Siberian Arctic during the past three glacial-interglacial cycles, J. Paleolimnol., 37, 89–104, 2007.
Minyuk, P. S., Brigham-Grette, J., Melles, M., Borkhodoev, V. Y., and Glushkova, O. Y.: Inorganic geochemistry of El'gygytgyn Lake sediments northeastern Russia as an indicator of paleoclimatic change for the last 250 kyr, J. Paleolimnol., 37, 123–133, 2007.
Nolan, M.: Analysis of local AWS and NCEP/NCAR reanalysis data at Lake Elgygtytgyn, and its implications for maintaining multi-year lake-ice covers, Clim. Past Discuss., 8, 1443–1483, doi:10.5194/cpd-8-1443-2012, 2012.
Nolan, M. and Brigham-Grette, J.: Basic hydrology, limnology, and meteorology of modern Lake El'gygytgyn, Siberia, J. Paleolimnol., 37, 17–35, 2007.
Nolan, M., Liston, G., Prokein, P., Brigham-Grette, J., Sharpton, V., and Huntzinger, R.: Analysis of Lake Ice Dynamics and Morphology on Lake El'gygytgyn, Siberia, using SAR and Landsat, J. Geophys. Res., 108, 8162, doi:10.1029/2001JD000934, 2003.
Reusch, D. B., Hewitson, B. C., and Alley, R. B.: Towards ice core-based synoptic reconstructions of West Antarctic climate with artificial neural networks, Int. J. Climatol., 25, 581–610, 2005.
Schuenemann, K. and Cassano, J. J.: Changes in synoptic weather patterns and Greenland precipitation in the 20th and 21st centuries, Part 2: Analysis of 21st century atmospheric changes using self-organizing mps, J. Geophys. Res., 115, D05108, doi:10.1029/2009JD011706, 2010.

CPD
8, 1485–1522, 2012

Table 1. The first three columns represent the three terms in Eq. (5). “Ratio” is the ratio of thermodynamics to frequency (that is, Term 1 divided by Term 2), DD_2-DD_1 is the change in degree days calculated in Eq. (5) (the sum of the three Terms).

	Thermo-dynamics (Term 1)	Frequency (Term 2)	Combined (Term 3)	Ratio	DD_2-DD_1
MAM	341.8	−24.9	21.6	13.7	338.4
JJA	24.1	8.5	−1.9	2.8	30.6
SON	324.3	1.1	−7.9	294.8	317.5
DJF	196.9	−33.6	35.6	5.8	199.1
Annual	887.2	−48.7	47.4	18.2	886

CPD
8, 1485–1522, 2012

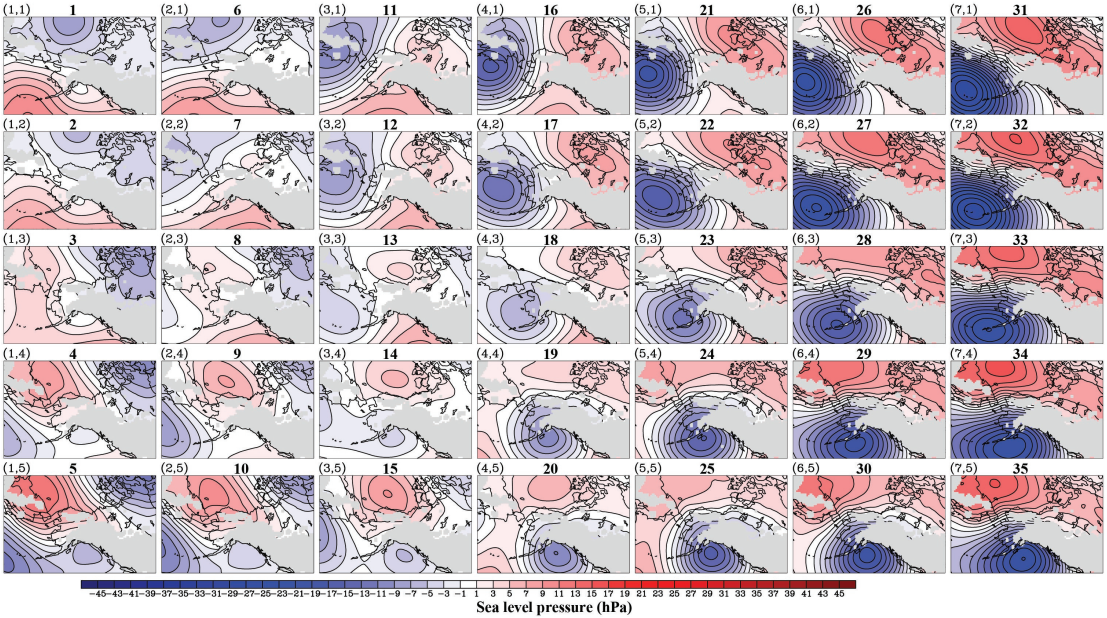

Fig. 1. SOM map used in this study. Numbers 1–35 and (column,row) indicate the two methods used to label patterns in subsequent figures and in the text.

CPD
8, 1485–1522, 2012

Synoptic climatology and recent climate trends at Lake El'gygytgyn

M. Nolan et al.

Title Page
Abstract | Introduction
Conclusions | References
Tables | Figures
◀ | ▶
Back | Close
Full Screen / Esc
Printer-friendly Version
Interactive Discussion

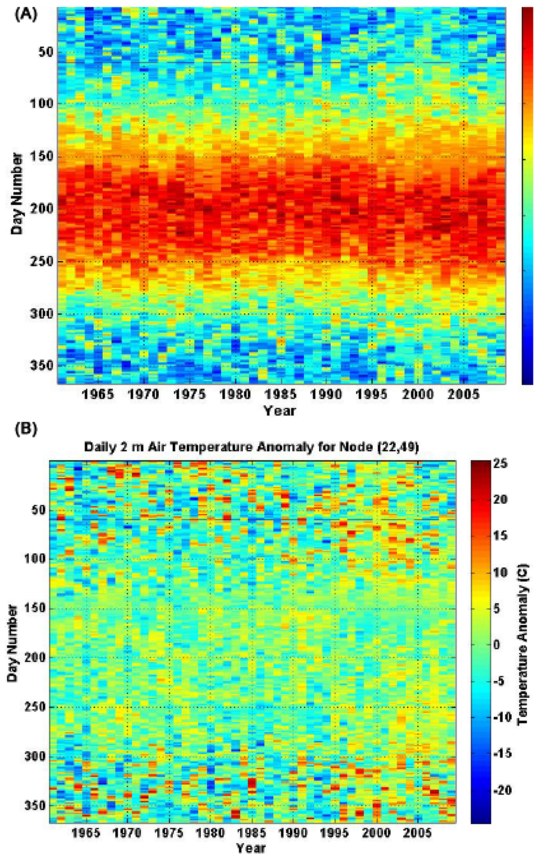

Fig. 2. (A) Daily NNR air temperatures. **(B)** Daily NNR air temperatures anomalies.

CPD
8, 1485–1522, 2012
Synoptic climatology and recent climate trends at Lake El'gygytgyn
M. Nolan et al.

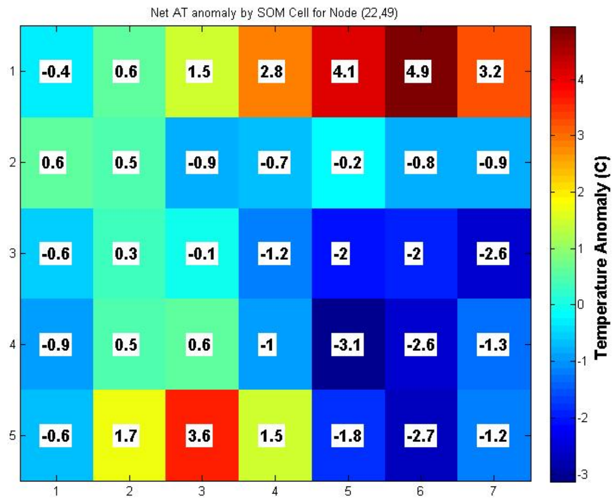

Fig. 3a. Pattern-averaged temperature anomaly for the NNR node closest to Lake El'gygygytgyn.

CPD
8, 1485–1522, 2012

Synoptic climatology and recent climate trends at Lake El'gygytgyn

M. Nolan et al.

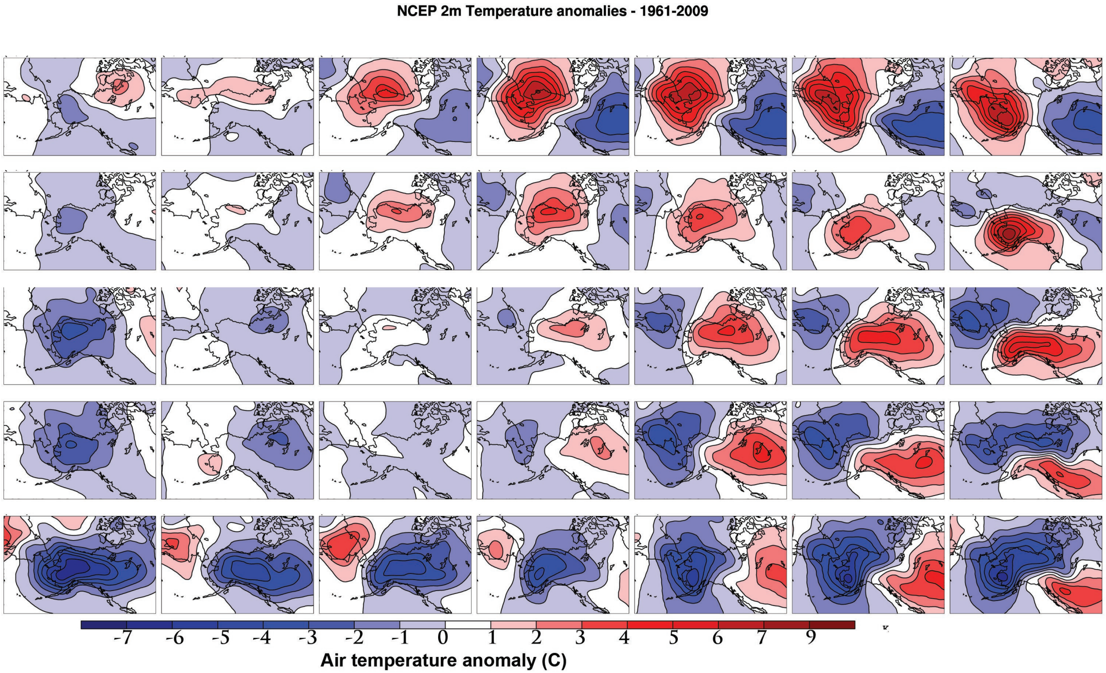

Fig. 3b. Temperature anomalies for each SOM pattern for each NNR node across the entire domain.

CPD
8, 1485–1522, 2012

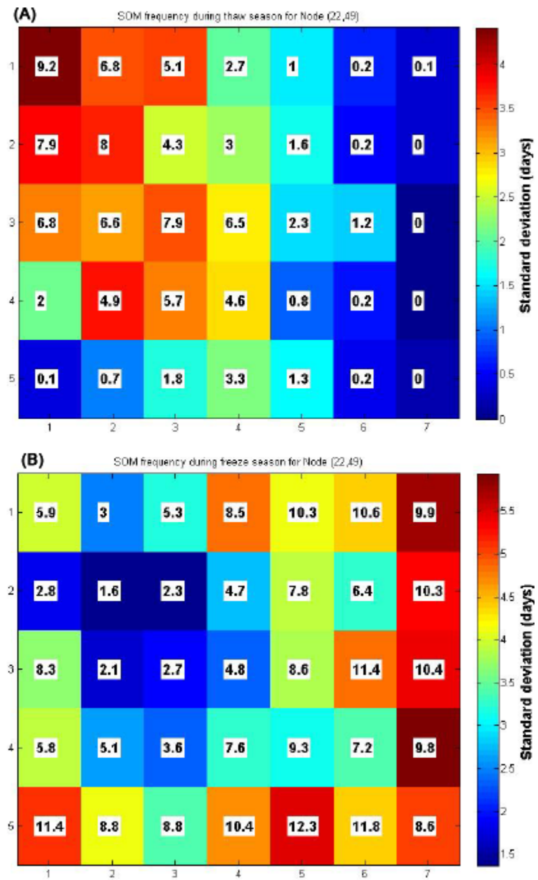

Fig. 4. (A) Mean SOM pattern frequencies in days per year (text) and their standard deviations (color) during the thaw season from 1961–2009. **(B)** Mean SOM pattern frequencies in days per year (text) and their standard deviations (color) during the freeze season from 1961–2009.

CPD
8, 1485–1522, 2012

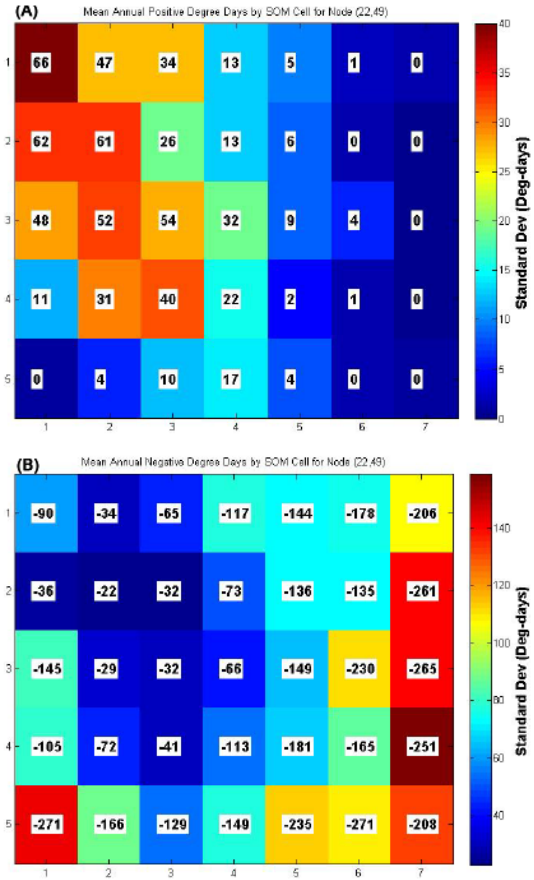

Fig. 5. **(A)** Mean positive degree days for each SOM pattern over 1961–2009. **(B)** Mean negative degree days for each SOM pattern over 1961–2009.

CPD
8, 1485–1522, 2012

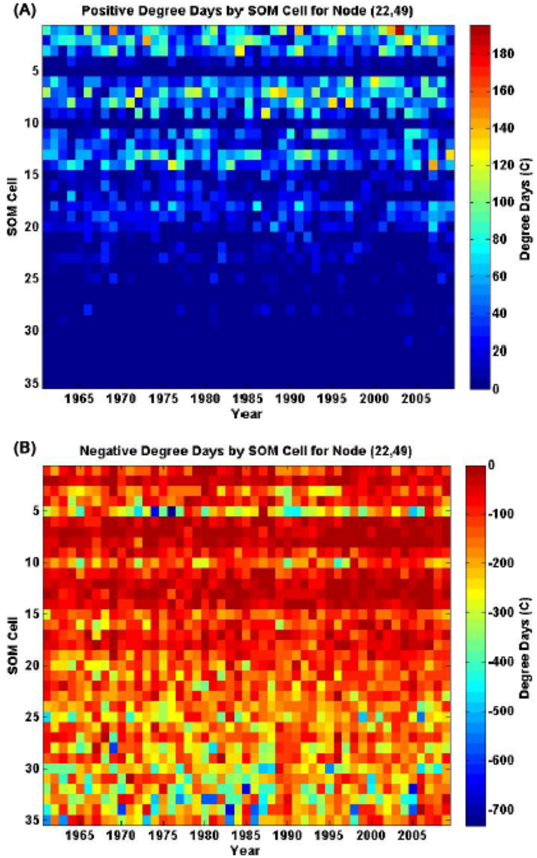

Fig. 6. (A) Positive degree days by SOM pattern (1–35) for each year of the NNR record. **(B)** Negative degree days by SOM pattern (1–35) for each year of the NNR record.

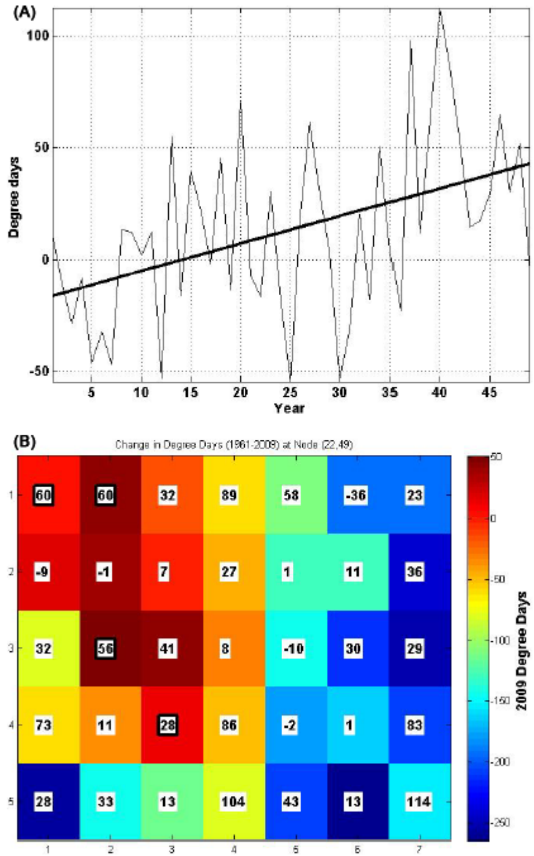

Fig. 7. **(A)** Change in degree days 1961–2009 for SOM pattern 6 with trend line (thick line). **(B)** Change in degree days 1961–2009 for all SOM patterns.

CPD
8, 1485–1522, 2012

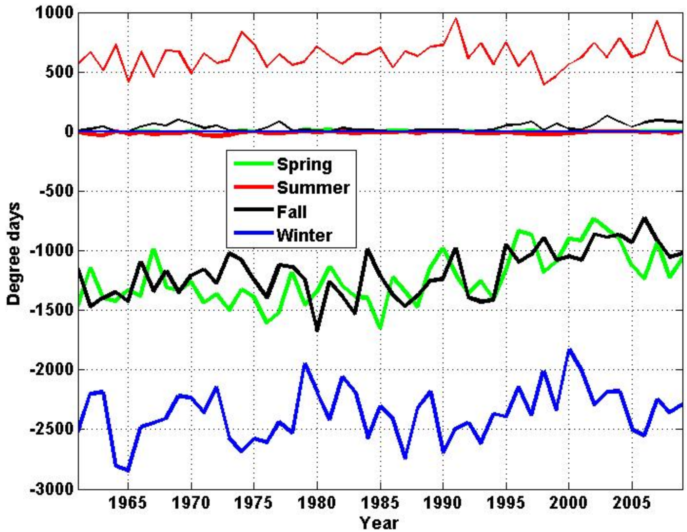

Fig. 8. Seasonal variations of PDD (thin lines) and NDD (thick lines).

CPD
8, 1485–1522, 2012

Synoptic climatology and recent climate trends at Lake El'gygytgyn

M. Nolan et al.

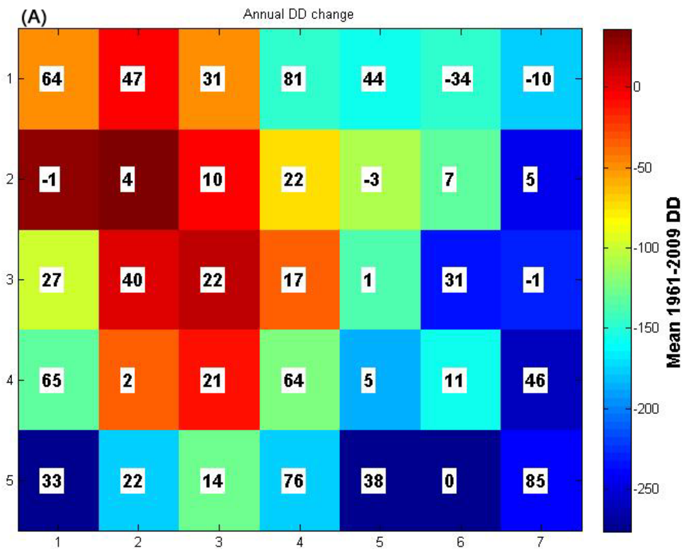

Fig. 9a. See caption on p. 1519.

CPD
8, 1485–1522, 2012

Synoptic climatology and recent climate trends at Lake El'gygytgyn

M. Nolan et al.

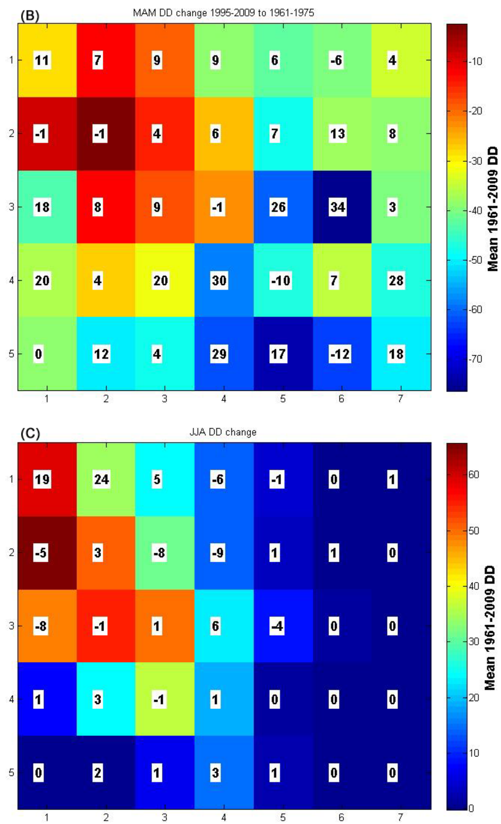

Fig. 9b and c. See caption on next page.

CPD
8, 1485–1522, 2012

Synoptic climatology and recent climate trends at Lake El'gygytgyn

M. Nolan et al.

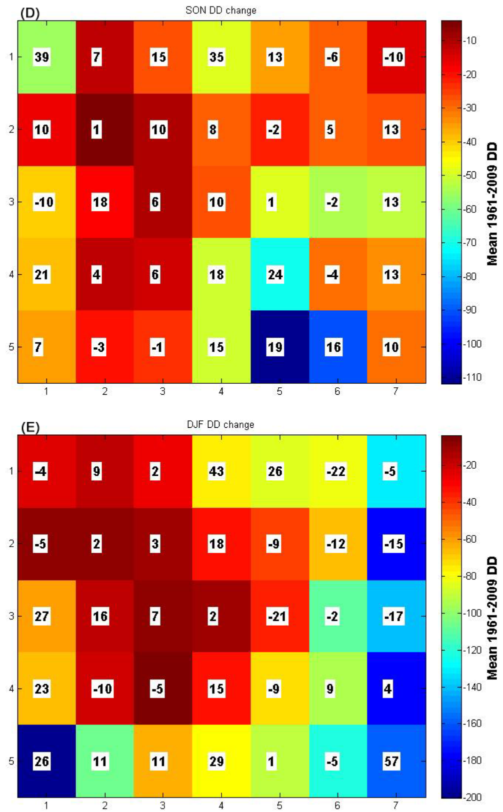

Fig. 9d and e. **(A)** Annual changes in degree days between 1995–2009 and 1961–1975. Note that nearly all patterns are showing warming. **(B)** MAM (spring) and **(C)** JJA (summer) changes in degree days between 1995–2009 and 1961–1975. **(D)** SON (fall) and **(E)** DJF (winter) changes in degree days between 1995–2009 and 1961–1975.

CPD
8, 1485–1522, 2012

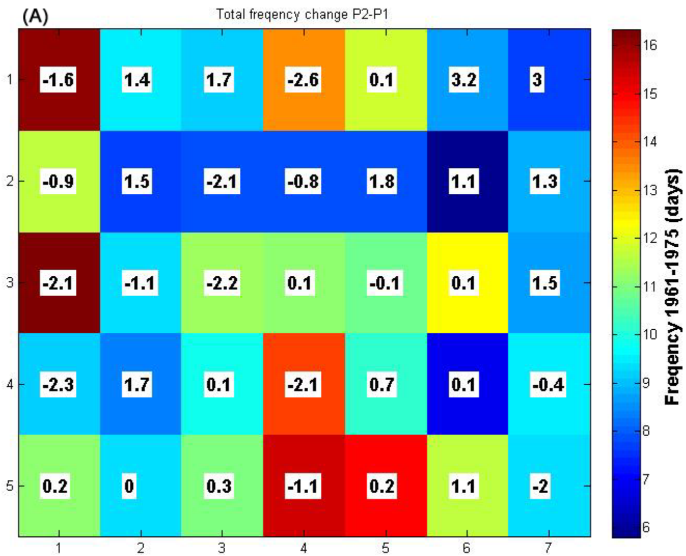

Fig. 10a. See caption on p. 1522.

CPD
8, 1485–1522, 2012

Synoptic climatology and recent climate trends at Lake El'gygytgyn

M. Nolan et al.

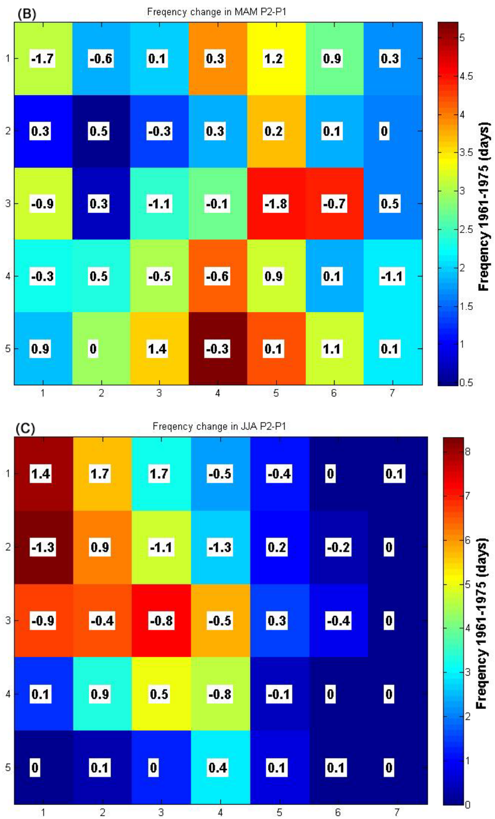

Fig. 10b and c. See caption on next page.

CPD
8, 1485–1522, 2012

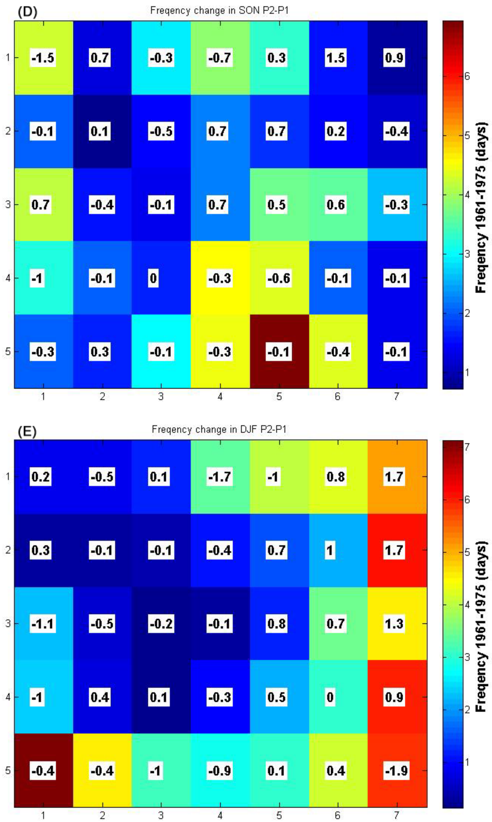

Fig. 10d and e. Change in average pattern frequency between 1995–2009 and 1961–1975. Text shows change in days, colors show pattern frequency during the first period in days. **(A)** Annual, **(B)** MAM, **(C)** JJA, **(D)** SON, and **(E)** DJF.

CPD

8, 1485–1522, 2012

Synoptic climatology and recent climate trends at Lake El'gygytgyn

M. Nolan et al.